Steady-State Electric Field and Conductivity in Mass-Impregnated HVDC Cable Insulation

Copyright for the article
© 2018 IEEE

The accepted version of the article starts on the following page.

The final, published version of the article is available here:
https://ieeexplore.ieee.org/document/8514639

Citation:
Gunnar Håkonseth and Erling Ildstad, "Steady-State Electric Field and Conductivity in Mass-Impregnated HVDC Cable Insulation," *2018 IEEE 2nd International Conference on Dielectrics (ICD)*, Budapest, 2018.

Digital Object Identifier (DOI)
10.1109/ICD.2018.8514639

Changes from the accepted version to the final, published version

- No changes in text and figures.

Errata for both the accepted version and the final, published version

- Caption to Figure 4:
  Replace $a = 7.81 \times 10^{-15}$ S/m with $a = 1.49 \times 10^{-16}$ S/m.
  Replace $b = 3.00 \times 10^{-8}$ m/V with $b = 3.02 \times 10^{-8}$ m/V.
- Caption to Figure 5:
  Replace $a = 1.87 \times 10^{-16}$ S/m with $a = 4.72 \times 10^{-15}$ S/m.
  Replace $b = 2.63 \times 10^{-8}$ m/V with $b = 3.03 \times 10^{-8}$ m/V.
- Caption to Figure 6:
  E_m/E_p should be E_p/E_m.

This version of this front page was made on August 12, 2019.

Steady-State Electric Field and Conductivity in Mass-Impregnated HVDC Cable Insulation

Gunnar Håkonseth*
Nexans Norway AS
PO Box 42
NO-1751 Halden
Norway
Email: gunnar.hakonseth@nexans.com

Erling Ildstad
Norwegian University of Science and Technology (NTNU)
Department of Electric Power Engineering
NO-7491 Trondheim
Norway
Email: erling.ildstad@ntnu.no

*Also with NTNU, Department of Electric Power Eng.

***Abstract*—This paper presents results from measurements and calculations of the steady-state DC electric field and the field-dependent conductivity in the two insulation materials found in mass-impregnated HVDC cables: Cable mass (a high-viscosity mineral oil) and paper that is impregnated with that mass. An important assumption for the work was that the relationship between the electric fields in the two materials depends only on the relationship between their conductivities. It was found that the conductivity of the mass is 2–5 times higher than the conductivity of the impregnated paper during normal, steady-state conditions in cables. Consequently, the electric field in the impregnated paper is 2–5 times higher than the electric field in the mass under such conditions.**

***Keywords*—power cable insulation; oil filled cables; underwater cables**

I. Introduction

The electric insulation in mass-impregnated high voltage direct current cables consists of approximately 2 cm wide and 0.09 mm thick paper strips that are helically wrapped around the conductor of the cable. The pitch of the helices is chosen so that a gap is left between adjacent windings. These gaps, which are called "butt gaps" and are about 2 mm wide, permits bending of the cable. Each layer of paper strips is staggered with respect to the layer below, so that the butt gaps in the two neighboring layers are not placed directly above each other. The paper is impregnated with an high-viscosity impregnation compound, the so-called called "mass". The mass consists of a mineral oil with thickeners and other additives. The mass fills the internal, fibrous structure of the paper, as well as the butt gaps and interfaces between the paper strips.

In the following, the impregnated paper is regarded as a homogeneous material. The internal structure of cellulose fibers and mass inside the paper is neglected. Consequently, the insulation is regarded as a composite of two materials:

- impregnated paper strips, i.e. cellulose fibers with mass in between the fibers, in the following denoted just "paper"
- mass in the butt gaps between the paper strips

A sketch of the insulation is shown in Fig. 1.

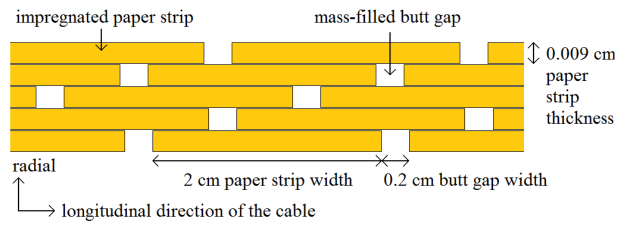

Fig. 1. Model of mass-impregnated HVDC cable insulation. Approximate dimensions. The sketch is not to scale.

As will be shown below, the electric field distribution in the different materials of the insulation under steady-state DC conditions are governed by the ratio between the conductivity of the mass and the conductivity of the paper. This article presents results from measurements of the conductivity in paper and mass, and computations of corresponding electric fields in geometries relevant to mass-impregnated HVDC cables.

No attention is payed to the charging process of the dielectric systems, where the electric field distribution is mainly governed by the rate of change of the displacement field instead of the conductivities, and where the currents are different from the steady-state DC current. In the following, the term *current* means *steady-state DC current*. Consequently, *current density* means *steady-state DC current density*.

II. Theory

A. Conductivity and Electric Field Distribution

1) Capacitor with One Dielectric Material: Here, a parallel plate capacitor containing a single, homogeneous material of thickness d and area A is considered. Any possible alteration

This work is part of the project "Mass Impregnated Non-Draining HVDC Submarine Cables" led by Nexans Norway AS. The project is financially supported by The Research Council of Norway (Norges forskningsråd), Nexans Norway AS, Statnett SF, Affärsverket svenska kraftnät, and Fingrid Oyj, and has project number 256405/E20 within the ENERGIX program of The Research Council of Norway.

978-1-5386-6389-9/18/$31.00 ©2018 IEEE

of the conductivity in the vicinity of the electrodes due to charge injection is assumed to be negligible, and edge effects are neglected.

The electric field E in the dielectric when the capacitor is subjected to a DC voltage U is then

$$E = U/d. \tag{1}$$

The conductivity σ is

$$\sigma = J/E, \tag{2}$$

where J is the steady-state current density in the dielectric.

2) Capacitor with Two Dielectric Materials: Now a parallel plate capacitor of two homogeneous, dielectric materials is considered. The materials are numbered 1 and 2, respectively. The same assumptions as above are maintained. Furthermore, it is assumed that there is no transition zone between the materials, and that the materials are in perfect electrical contact with each other. The thicknesses of material 1 and 2 are $d_{1,2}$ and the conductivities $\sigma_{1,2}$, respectively.

Equation (2) holds for each material separately, so that $\sigma_1 = J_1/E_1$ and $\sigma_2 = J_2/E_2$. Since $J_1 = J_2$ at steady-state conditions, we have

$$\frac{E_1}{E_2} = \frac{\sigma_2}{\sigma_1}. \tag{3}$$

The electric field in material 1 when the capacitor has been subjected to a DC voltage U for a sufficiently long time for steady-state DC conditions to occur, is then [1]

$$E_1 = \frac{U\sigma_2}{d_1\sigma_2 + d_2\sigma_1}. \tag{4}$$

Sometimes it is convenient to express (4) as

$$E_1 = \frac{\bar{E}(\frac{d_1}{d_2}+1)\sigma_2}{\frac{d_1}{d_2}\sigma_2 + \sigma_1} \tag{5}$$

where $\bar{E} = U/(d_1 + d_2)$ is the mean field strength.

The electric field E_2 in the other material can be found by swapping the indices 1 and 2 in (4), or by using the relation

$$E_2 = \frac{U - d_1E_1}{d_2}. \tag{6}$$

B. Methods of Conductivity Measurements

1) Method 1—One Material: The conductivity of a material may depend on the electric field in that material [2]. For a material as in section II-A1, an empirical formula for $\sigma(E)$ can be found in this way:

1) Perform measurements of J at different values of U.
2) Use (1) and (2) to find E and σ.
3) Curve fit to obtain an empirical formula for $\sigma(E)$.

2) Method 2—Two Materials in a Series Connection: In case of a series connection of two materials as in section II-A2 where the field-dependent $\sigma_1(E_1)$ for material 1 is known, we can obtain an empirical formula for material 2 in this way:

1) Perform measurements of J at different values of U.
2) For each J, insert an already known formula for $\sigma_1(E_1)$ into (2) and solve for E_1.
3) For each E_1, use (6) to find E_2.
4) For each E_2, use (2) to find σ_2.
5) Curve fit to obtain an empirical formula for $\sigma(E_2)$.

If $\sigma_1(E_1)$ is not field-dependent, the solution of (2) in step 2) is trivial, and steps 2) through 4) can for each J be replaced by the formula

$$\sigma_2 = \frac{J\sigma_1 d_2}{\sigma_1 U - Jd_1}. \tag{7}$$

On the other hand, if $\sigma_1(E_1)$ is field-dependent, (2) can be more difficult to solve. However, if $\sigma_1(E_1)$ is an exponential relation

$$\sigma_1(E_1) = a\exp(bE_1) \tag{8}$$

where a and b are constants, the solution of (2) is

$$E_1 = \frac{\mathrm{W}_0(z)}{b}, \tag{9}$$

where W_0 is the principal branch of the Lambert W function [3], and its argument $z = Jb/a$. Then, steps 2) through 4) can for each J instead be replaced by the formula

$$\sigma_2 = \frac{d_2bJ}{bU - d_1\mathrm{W}_0(z)}. \tag{10}$$

III. Experimental Method

Cable paper sheets of nominal thickness 90 µm were dried in vacuum at 100–120 °C for minimum 48 hours. Mass was degassed by circulating in another vacuum chamber at approx. 100 °C for at least 4 hours. The degassed mass was transferred through a piping system to the vacuum chamber containing the paper sheets. The mass completely covered the paper sheets before the paper-containing chamber was opened and the electrode arrangement was put in place around the sample. Then the chamber was quickly closed and flushed with dry nitrogen before the whole arrangement was left for the temperature to stabilize. The temperatures used for measurements were 22 °C and 50 °C. Voltages up to $U = 35\,\mathrm{kV}$ were used, giving mean field strengths up to $\bar{E} = 25.7\,\mathrm{kV/mm}$.

Three types of samples were used:

- "Paper sample":
  A stack of four or five paper sheets.
- "Series connection sample":
  A stack of four paper sheets with a mass-filled gap of 1 mm in the middle of the stack.
- "Mass sample":
  An 1 mm section of mass, without any paper.

The stack thickness was assumed to be the nominal thickness of one sheet multiplied with the number of sheets in the stack. The mass samples and the gap in the series connection samples were made by using a polytetrafluoroethylene spacer. The samples and the electrode arrangement were surrounded by mass. The electrodes were circular and made of brass. They were connected to a DC source (Fug HCN 140 - 35 000) and a picoamperemeter (Keithley 6485), as well as equipment for protecting and controlling the circuit. A sketch of the electrode arrangement and the circuit is shown in Fig. 2.

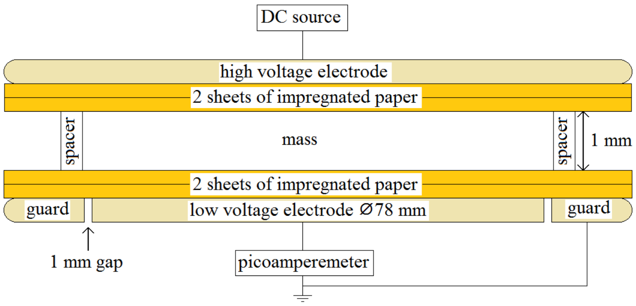

Fig. 2. Cross-sectional sketch of the electrode arrangement used for measuring series connection of paper and mass. The figure is not to scale.

The current was measured at least until the rate of change was less than 7 % per hour for the paper samples and the series connection samples, and 7 % per 1000 s for the mass samples.

The field-dependent conductivity $\sigma_\mathrm{p}(E_\mathrm{p})$ of paper was measured using Method 1 with the paper samples. Subsequently, the field-dependent conductivity $\sigma_\mathrm{m}(E_\mathrm{m})$ of mass was measured with both methods from section II-B in two different ways: Method 1 with the mass samples, and Method 2 with the series connection samples (with $\sigma_\mathrm{p}(E_\mathrm{p})$ from Method 1 as input to the computations).

When $\sigma_\mathrm{p}(E_\mathrm{p})$ and $\sigma_\mathrm{m}(E_\mathrm{m})$ were found, E_p and E_m were estimated for geometries and mean field strengths relevant to HVDC cables. Instead of using (4), which was difficult or impossible to use because of the field-dependence of the conductivities, the finite element method (FEM) was used. The FEM software *Comsol Multiphysics 5.3* was used to create an one-dimensional model of paper and mass in a series connection. The software was set to solve (2) together with $E = -\nabla V$ and $\nabla \cdot J = 0$, where V is the electric potential. The different field-dependencies of $\sigma_\mathrm{p}(E_\mathrm{p})$ and $\sigma_\mathrm{m}(E_\mathrm{m})$ were taken into account. This yielded values for the conductivities and the fields for different values of d_p, d_m, and $\bar{E}$.

IV. Results

A. Method 1—Paper Samples and Mass Samples

Fig. 3 shows the measured conductivity in paper samples and mass samples at 50 °C, obtained with the method described in section II-B1. The results for mass had poor repeatability compared with that of the paper. It was not possible to measure the mass samples at higher field strengths than $7\,\mathrm{kV/mm}$ because the DC source and picoamperemeter showed signs of electrical breakdown in the sample. For field strengths up to $7\,\mathrm{kV/mm}$, the highest σ_m was 20 times higher than the lowest σ_p, and the lowest σ_m was 2 times higher than the highest σ_p.

The sample of five paper sheets was measured at 22 °C and 50 °C with field strengths from 11 to $56\,\mathrm{kV/mm}$, still using the method described in section II-B1. Curve fitting those results to $\sigma_\mathrm{p}(E_\mathrm{p}) = a\exp(bE_\mathrm{p})$ gave $a = 1.49 \times 10^{-16}\,\mathrm{S/m}$ and $b = 3.02 \times 10^{-8}\,\mathrm{m/V}$ for 22 °C, and $a = 4.72 \times 10^{-15}\,\mathrm{S/m}$ and $b = 3.03 \times 10^{-8}\,\mathrm{m/V}$ for 50 °C.

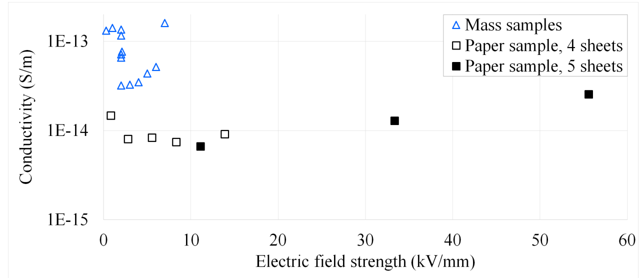

Fig. 3. Conductivity in mass samples and paper samples at 50 °C. Equation 2 was used.

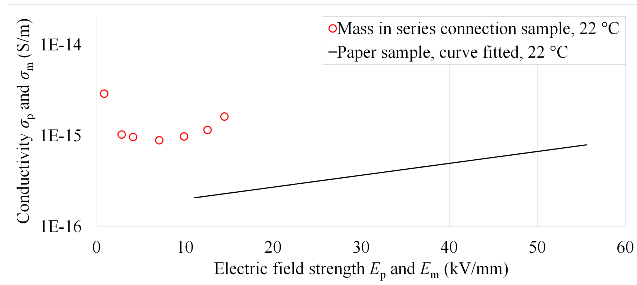

Fig. 4. Conductivity of mass in the series connection sample at 22 °C. The solid line shows $\sigma_\mathrm{p}(E_\mathrm{p}) = a\exp(bE_\mathrm{p})$ with $a = 7.81 \times 10^{-15}\,\mathrm{S/m}$ and $b = 3.00 \times 10^{-8}\,\mathrm{m/V}$, which was used for computing E_m.

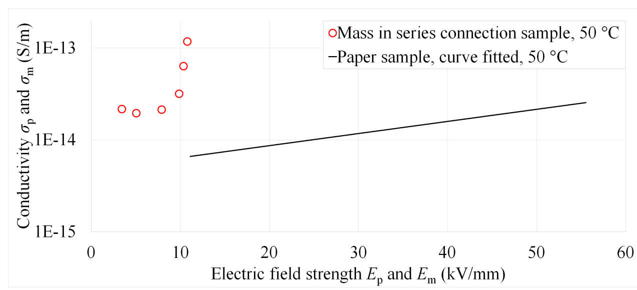

Fig. 5. Conductivity of mass in the series connection sample at 50 °C. The solid line shows $\sigma_\mathrm{p}(E_\mathrm{p}) = a\exp(bE_\mathrm{p})$ with $a = 1.87 \times 10^{-16}\,\mathrm{S/m}$ and $b = 2.63 \times 10^{-8}\,\mathrm{m/V}$, which was used for computing E_m.

B. Method 2—Series Connection Samples

Fig. 4 and 5 show results from measurements of σ_m in series connection samples at 22 °C and 50 °C, respectively. These results were obtained by using $\sigma_\mathrm{p}(E_\mathrm{p}) = a\exp(bE_\mathrm{p})$ as presented above, together with the procedure described in section II-B2. Note that σ_p was not *measured* with this method, but was used as input to the computation of E_m and σ_m.

Fig. 6 shows computations of the ratio $E_\mathrm{m}/E_\mathrm{p}$ in series couplings of paper and mass with with various mean field strengths and ratios of $d_\mathrm{p}/d_\mathrm{m}$. In the series coupling samples, $d_\mathrm{p}/d_\mathrm{m}$ was $4/11$. In cables, $d_\mathrm{p}/d_\mathrm{m}$ depends on how many paper strips there are between butt gaps in the radial direction. The computations were done with *Comsol Multiphysics*.

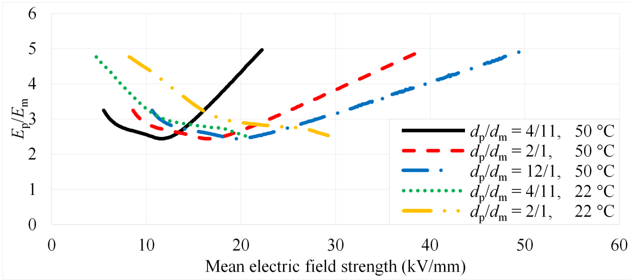

Fig. 6. E_m/E_p as functions of mean electric field strength $\bar{E}$ for various ratios of total paper thickness to mass thickness (d_p/d_m). In the series connection samples, d_p/d_m was 4/11.

V. Discussion

For $E \leq 7\,\text{kV/mm}$ at 50 °C, results from measurements of σ_m with Method 1 are in the range from 3.2×10^{-14} to 1.6×10^{-13}. This is 2–20 times higher than σ_p obtained with the same method at the same field strengths. Note that this comparison of $\sigma_p(E_p)$ and $\sigma_m(E_m)$ is done with $E_p = E_m$. The dispersion in σ_m is pronounced, and there is no clear trend for σ_m as a function of E_m.

Method 2 at the same temperature gave lower and approximately constant values for $\sigma_m(E_m)$ for the same range of E_m. The lower values could possibly be due to less effective change of polarity of charge carriers in the mass at the mass–paper interfaces in the series coupling samples than at the mass–brass interfaces in the mass samples. If charge carriers change polarity without being trapped when meeting an interface, they can start going in the opposite direction and continue to contribute to the current. It should be noted that although the mass gap was designed to be between the paper sheets, the upper and lower paper stacks had a tendency to attract each other. In some of the experiments much of the mass may therefore have been between a paper stack and the brass electrode, instead of between the upper and lower paper stack. Nevertheless, the mass samples had no mass–paper interfaces, whereas the series connection samples had at least one mass–paper interface. In a cable, the butt gaps are surrounded by paper, and the series connection samples resemble this situation better than the mass samples do. Electrical breakdown was not a problem in the series coupling samples.

At approximately $10\,\text{kV/mm}$, where Method 1 did not work, σ_m started to increase.

Method 2 gave similar results at 22 °C as at 50 °C, but σ_p and σ_m at 22 °C were less than 5 % of the corresponding values for 50 °C (Fig. 4), and the highest value of σ_m at 22 °C was obtained at the lowest field strength. Due to limitations of the DC voltage source, E_m in the series connection samples did not exceed $14.5\,\text{kV/mm}$ at 22 °C and $10.8\,\text{kV/mm}$ at 50 °C. Below these field strengths, the ratio σ_m/σ_p never exceeded 20. Both at 22 °C and 50 °C, $\sigma_m(E_m)$ starts to increase with E_m at approximately $10\,\text{kV/mm}$. Extrapolations based on the slopes of $\sigma_m(E_m)$ for both temperatures suggest that at higher field strengths than obtained in the present work, the ratio σ_m/σ_p would be larger. Also here, the comparison of $\sigma_p(E_p)$ and $\sigma_m(E_m)$ is done with $E_p = E_m$.

Up to now we have compared $\sigma_m(E_m)$ with $\sigma_p(E_p)$ where $E_m = E_p$. This is not the situation in a real capacitor or a real cable, where $E_p/E_m = \sigma_m/\sigma_p$. Since $\sigma_m > \sigma_p$, we have $E_p > E_m$. This means that $\sigma_p(E_p)$ has to be evaluated at a higher field strength than $\sigma_m(E_m)$, and the field-dependencies of the conductivities have a restraining effect on the ratio E_p/E_m. Typical mean field strengths in HVDC cable insulation during steady-state conditions are in the range of $10–40\,\text{kV/mm}$ [2]. The results presented in Fig. 6 shows that the ratio E_p/E_m is expected to be between 2 and 5 in such cases. Therefore, extrapolations of E_m as mentioned above appear not to be necessary for calculation of the local electric fields in mass-impregnated HVDC cables.

Fig. 6 was made under the assumption that neither of the conductivities depend on the thickness of the dielectric. It follows from the same assumption and (5) that the curves in Fig. 6 would not change if d_p and d_m were changed, as long as the ratio between those parameters were kept constant. It is known that the size of the oil gap can influence the apparent conductivity in liquid dielectrics [4]. This suggests that the effect of d_p and d_m need to be investigated.

VI. Conclusion

The ratio $\sigma_m(E_m)/\sigma_p(E_p)$, where E_m and E_p are the actual electric fields in the respective materials during operation of mass-impregnated HVDC cables, were found to be between 2 and 5 for mean electric field strengths normally present at steady-state conditions in such cables. Consequently, E_p/E_m is also between 2 and 5 at the same conditions.

Acknowledgments

The authors want to thank colleagues at Nexans Norway AS, The Norwegian University of Science and Technology (NTNU), and SINTEF Energy Research for practical help and discussions. In particular, the authors want to mention Knut Magne Furuheim, Øystein Leif Gurandsrud Hestad, Knut Brede Liland, Dag Linhjell, Frank Mauseth, Lars Erik Pettersen, and Torbjørn Andersen Ve.

References

[1] F. H. Kreuger, *Industrial high DC voltage: 1. fields, 2. breakdowns, 3. tests*. Delft: Delft Univ. Press, 1995.

[2] M. J. P. Jeroense, "Charges and discharges in HVDC cables: in particular in mass-impregnated HVDC cables," Ph.D. dissertation, Delft University Press, Delft, 1997.

[3] R. M. Corless, G. H. Gonnet, D. E. G. Hare, D. J. Jeffrey, and D. E. Knuth, "On the Lambert W function," *Advances in Computational Mathematics*, vol. 5, no. 1, pp. 329–359, Dec. 1996.

[4] M. E. Z. Eldine, A. A. Zaky, R. Hawley, and M. C. Cullingford, "Influence of insulating films on conduction," *Proceedings of the Institution of Electrical Engineers*, vol. 112, no. 3, pp. 580–585, Mar. 1965.